

The AEI 10 m Prototype Interferometer frequency control using the reference cavity and its angular control

Fumiko Kawazoe¹, Gerald Bergmann¹, Alessandro Bertolini²,
Michael Born¹, Yanbei Chen³, Alan V. Cummning⁴,
Liam Cunningham⁴, Katrin Dahl¹, Christian Gräf¹, Giles Hammond⁴,
Gerhard Heinzel¹, Stefan Hild⁴, Sabina H. Huttner⁴, Russell Jones⁴,
Sina Köhlenbeck¹, Gerrit Kühn¹, Harald Lück¹, Kasem Mossavi¹,
Jan Hendrik Pöld¹, Kentaro Somiya⁵, A. Marielle van Veggel⁴,
Alexander Wanner¹, Tobias Westphal¹, Benno Willke¹,
Kenneth Strain^{1,4}, Stefan Goßler¹, and Karsten Danzmann¹

¹ Max-Planck-Institut für Gravitationsphysik (Albert-Einstein-Institut) und Leibniz
Universität Hannover, Callinstr. 38, D-30167 Hannover, Germany

² National Institute for Subatomic Physics, Science Park 105, 1098 XG Amsterdam,
Netherlands

³ California Institute of Technology, Pasadena, CA 91125 USA

⁴ University of Glasgow, Glasgow, G12 8QQ, United Kingdom

⁵ Tokyo Institute of Technology, 2-12-1 Ookayama, Meguro-ku, Tokyo 152-8550, Japan

E-mail: fumiko.kawazoe@aei.mpg.de

Abstract. The main purpose of the AEI 10 m Prototype is to reach and eventually surpass the Standard Quantum Limit at frequencies ranging from 20 Hz to 1 kHz with a 10 m arm-length Michelson interferometer named the sub-SQL interferometer. The frequency control system uses a 20 m optical path length triangular suspended cavity named the reference cavity, with the goal of suppressing frequency noise of the input laser to a level of $\sim 10^{-4}$ Hz/ $\sqrt{\text{Hz}}$ at 20 Hz rolling off to below 6×10^{-6} Hz/ $\sqrt{\text{Hz}}$ above 1 kHz. It is expected that tight angular control of the reference cavity's mirrors is necessary to reach this stringent requirement.

1. Introduction

In the AEI 10 m Prototype a 10 m arm-length Fabry-Perot Michelson interferometer called the sub-SQL interferometer will be installed [1]. Its objective is to first reach and finally surpass the Standard Quantum Limit (SQL) for 100 g mirror masses in a frequency band of 20 Hz to 1 kHz, with its highest sensitivity centered around 200 Hz. We aim to achieve this goal by suppressing all other noise sources well below the quantum noise, as shown in Fig. 1.

We set up several subsystems to tackle known noise sources; isolation tables with a seismic attenuation system will attenuate the ground motion by a factor of about 10^{-3} at 10 Hz in vertical and horizontal directions, a suspension platform interferometer will measure and correct the residual motions between these tables to the level of 10 nrad/ $\sqrt{\text{Hz}}$ at 10 mHz for angular motions and 100 pm/ $\sqrt{\text{Hz}}$ at 10 mHz for longitudinal motions [2], triple cascaded mirror suspensions with

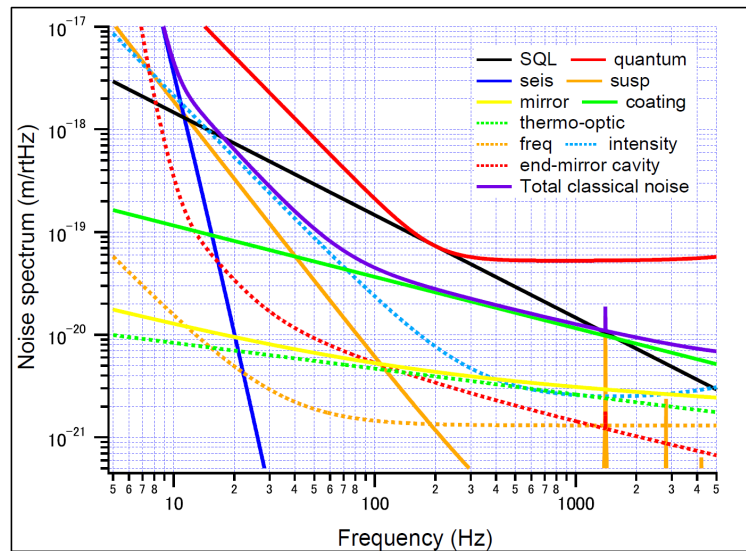


Figure 1. Design sensitivity of the sub-SQL interferometer.

an all silica monolithic last stage will minimize suspension thermal noise, and the frequency control system will suppress the laser frequency noise to a level of $\sim 10^{-4} \text{ Hz}/\sqrt{\text{Hz}}$ at 20 Hz rolling off to below $6 \times 10^{-6} \text{ Hz}/\sqrt{\text{Hz}}$ above 1 kHz [3].

2. Frequency Control System

Figure 2 shows a schematic layout of the reference cavity. It is a triangular cavity consisting of two flat mirrors and a curved mirror. Two flat mirrors are located close together, (the distance between them is 0.3 m) and the curved mirror is located ~ 10 m away from the flat mirrors. The cavity has an optical path length of ~ 20 m.

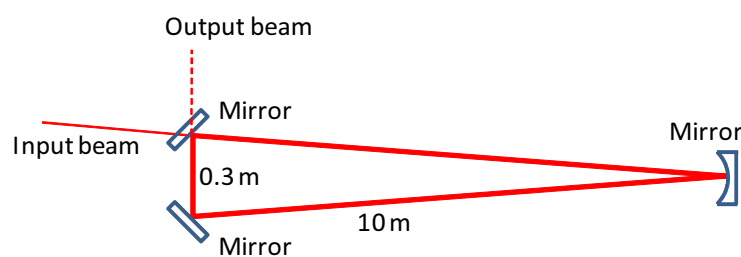


Figure 2. Schematic layout of the frequency reference cavity.

An asymmetry between the two arms of the sub-SQL interferometer can cause laser frequency noise to show up at the detection port. In our design we assume a common-mode rejection ratio of 99%. The laser is a 2 W InnoLight Mephisto non-planar monolithic ring oscillator (NPRO), which is amplified by a four head Nd:YVO₄ laser amplifier to a power level of 35 W [4]. Assuming the well known free running noise of an NPRO ($10^4 \text{ Hz}/\sqrt{\text{Hz}}$ at 1 Hz rolling off as $\propto 1/f$) [5] and the above mentioned common-mode rejection ratio, and adding a safety margin of ~ 10 , we set the target level of the frequency noise in the input beam to be $\sim 10^{-4} \text{ Hz}/\sqrt{\text{Hz}}$ at 20 Hz

dropping to below $6 \times 10^{-6} \text{ Hz}/\sqrt{\text{Hz}}$ at 1 kHz. Expressed in other units, this corresponds to a reference-cavity length-noise of $\sim 10^{-17}$ and $< 2 \times 10^{-19} \text{ m}/\sqrt{\text{Hz}}$, at $\sim 20 \text{ Hz}$ and $> 1 \text{ kHz}$, respectively. In Fig. 3 the free running noise of an NPRO and the target level are compared. This stringent suppression ratio requires us to set up a frequency reference cavity, and control the laser frequency to follow the cavity length fluctuations which are designed to be much smaller than the free running noise of the laser. The widely-adopted method to use a high-finesse arm cavity of the main interferometer (in this case, the sub-SQL) as a frequency reference fails in our case, as the arms are too susceptible to the radiation pressure noise. (The masses of the suspended mirrors for the sub-SQL will be 100 g while the power inside the arms will exceed 1 kW). A straightforward way to design a frequency reference cavity is to make its optical path

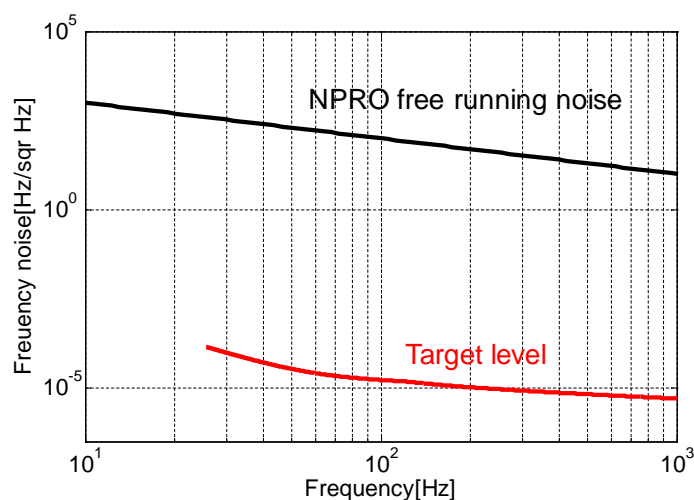


Figure 3. Target frequency noise level and a free running NPRO noise level.

length (L) long because given the minimum achievable displacement noise (ΔL), the frequency noise is proportional to $\Delta L/L$ and can be minimized by choosing the longest possible path length. The distance between two adjacent isolation tables being $\sim 10 \text{ m}$ allows an optical path length of order 20 m.

The mirror mass is 850 g, the substrate is made from Suprasil 2, the diameter is 10 cm, and the thickness is 5 cm. The mass is chosen as a compromise between the suspension thermal noise and the radiation pressure noise performance, and the load/space capacity of the isolation table. Note that the suspension system for each mirror weighs approximately 15 times more than the mirror itself.

With the mirror mass fixed, the power inside the reference cavity is optimized such that the radiation pressure noise and the shot noise level are well below the target level. The cavity finesse is optimized so that the value is high enough to have a reasonable signal to shot noise ratio, yet within experimental reach.

The beam radius of $\sim 2.5 \text{ mm}$ on the cavity mirrors is a compromise between the coating Brownian noise performance, and tolerance to optically induced torque and power fluctuations arising from angular fluctuations. The cavity g-factor is selected so that it is a non-degenerate cavity in which higher order spatial-modes are sufficiently suppressed. We assume that no more than 5% of the input power is distributed over those modes. Non-degeneracy will be important for the alignment control because the control signal depends on the different resonance conditions between the fundamental mode and higher order spatial-modes.

Table 1 shows the design parameters. Note that slight modifications to the early phase design parameters that are shown in [3] were made to compensate for the unpredictable manufacturing tolerances.

Table 1. Design parameters of the reference cavity.

Parameter	Specification
Optical path length	21.2 m
Input power	0.133 W
Finesse	7305
Circulating power	232 W
Higher order spatial-mode suppression for $n + m < 6$	>1000
Cavity g -factor	0.72
Beam waist size	2.4 mm
Mirror mass	850 g

With these parameters the calculated total noise of the reference cavity is at the same level as the target in the frequency range of interest, see Fig. 4. Several individual noise sources that are either limiting or close to limiting the total noise are plotted.

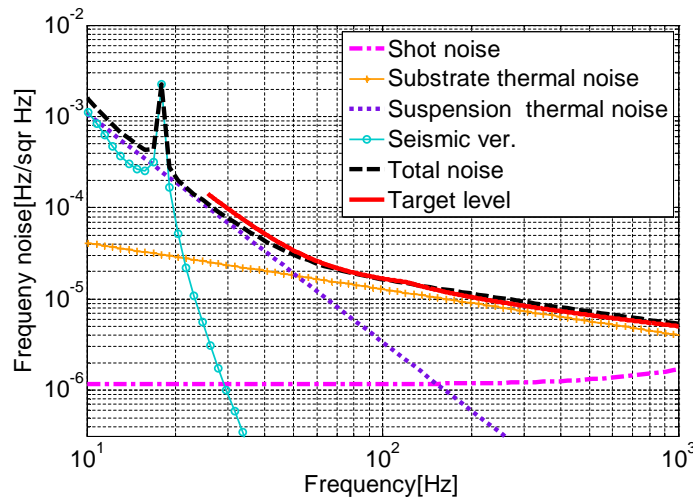


Figure 4. Noise budget of the reference cavity. The target level, the expected total noise level, and noise that are close to limiting the total noise of the reference cavity, and hence influence the cavity performance significantly, are shown.

In principle, if the NPRO frequency noise is suppressed to the target level within this frequency range our goal is achieved. In reality however, noise outside of this frequency range is expected to couple in through non-linear effects, e.g. scattering, and increase the total noise in the frequency range of interest. In order to prevent this we control the NPRO from below 1 Hz to the highest achievable frequency at which the phase lag in the control loop does not harm the control system's stability.

We take a common approach of using a Pound-Drever-Hall (PDH) technique, with several actuators that work in different frequency bands to cover the whole range: NPRO Temperature actuator, NPRO Piezoelectric Transducer(PZT), and a phase correcting Electro-optic Modulator (EOM). Figure 5 shows a block diagram for the feedback control system with the three actuators. Blue lines represent electrical signal path and the red dotted line represents the laser beam. The Laser Temperature feedback signal is picked up after the Laser PZT servo stage so that any changes to the PZT gain do not require consequential changes to the Laser Temperature gain to maintain a stable crossover condition. The bandwidth and the actuator coefficient of each

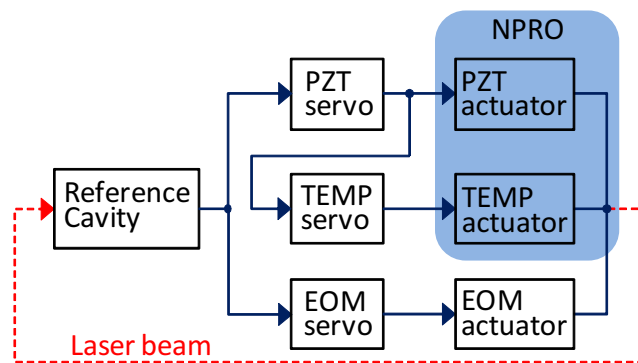


Figure 5. Block diagram for the feedback control system.

actuator are shown in Table 2. The unity gain frequency aimed at needs to include some safety margin because additional phase lag will arise from electronics, for example photo detectors, EOM driver, and post-mixer filters, that cannot be accurately predicted at this design phase. We aim at 250 kHz for the unity gain frequency at which the designed servo phase lag is less than 10 degrees.

Table 2. Design parameters of the reference cavity control.

Actuator	Bandwidth	Actuator coefficient
Laser Temperature	< 1 Hz	-3 GHz/V
Laser PZT	1 Hz - 10 kHz	1 MHz/V, Resonance at 200 kHz, $Q = 10$
Phase correcting EOM	10 kHz - 250 kHz	15 mrad/V

3. Angular control of the reference cavity

In order to maintain the full sensitivity, alignment degrees of freedom also need to be controlled. Otherwise they will introduce a drift in the system that will deteriorate the feedback control signal, making a robust control of the system impossible.

Three mirrors with two misalignment directions (horizontal and vertical) will give six degrees of freedom. A Differential Wavefront Sensing scheme (DWS) [6] and a Spot Position Control (SPC) will be used for controlling these degrees of freedom.

Wavefront misalignments appear as higher order spatial-modes that carry phase information that is different from that of the fundamental mode due to Gouy phase contributions. The DWS

uses a PDH technique with a split photo diode on which two segments detect opposite effects of a wavefront tilt, hence by taking a difference of the demodulated signals from each segment we obtain an error signal to feed back to the servo.

Combinations of four degrees of freedom of the reference cavity (see [7]), will define the tilt between wavefronts of the promptly reflected beam and the beam leaving the cavity, i.e. DWS is sensitive to them. On the other hand the remaining two degrees of freedom do not cause detectable changes, hence the effect of the promptly reflected beam and the beam leaving the cavity is the same, and will be detected as a spot position change on a position sensitive photo detector.

Two suspended steering mirrors will be placed in front of the reference cavity to act as actuation points for alignment control loops with a control bandwidth of up to a few Hz. In this way a faster control will be possible because the cavity mirrors are suspended as triple suspensions with no actuator at the mirror level while the steering mirrors use a single suspension stage allowing a direct actuation at the mirror level. For the SPC the cavity mirrors are used as actuators, with a control bandwidth up to 0.1 Hz. At frequencies below 0.1 Hz angular alignment of the remaining mirror degrees of freedom will be used for beam centering on the mirrors.

This control speed hierarchy is subject to change because of the lack of decisive factors in this design phase, e.g. it is not yet clear if the cavity mirror motions will create larger changes in the eigenmode than the steering mirror motions. However, it will not be a problem to change the hierarchy since it will only require minor changes in the experimental setup.

Figure 6 and 7 show a schematic overview of the alignment control of the DWS part and the SPC part, respectively. A modulation frequency of ~ 8 MHz is chosen so that the sidebands are

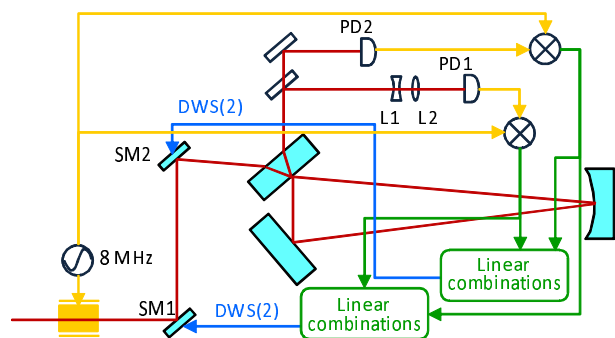


Figure 6. Schematic overview of the DWS part of the alignment control. (SM: steering mirrors, PD: quadrant photo detectors, L: lenses)

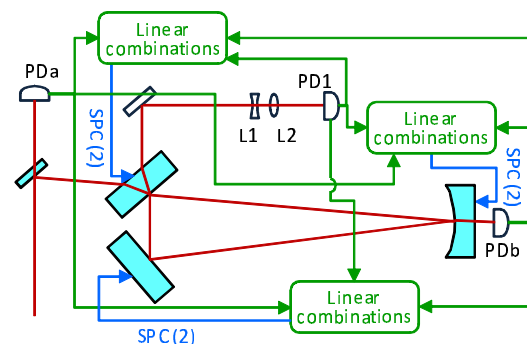


Figure 7. Schematic overview of the SPC part of the alignment control.

not resonant inside the cavity. For the SPC three photo detectors will detect six error signals and by taking proper linear combinations these signals will be fed back to the three cavity mirrors, and will be nulled via the DWS control. For the DWS, two photo detectors will create four demodulated signals and by taking proper linear combinations these signals will be fed back to the two steering mirrors, labeled SM1 and SM2. The number of degrees of freedom in the signals are denoted by the numbers in round brackets. L1 and L2 are widely called Gouy lenses, and are necessary for obtaining misalignment signals similar to those in the far field but at a much shorter distance than otherwise required. Figure 8 shows the overall layout of the reference cavity. The laser beam is sent into the vacuum tank through a fiber. The fiber and a Pre-Mode-Cleaner will give sufficient spatial mode filtering. Part of this spatially filtered beam will be sent into the reference cavity. All the detection systems will be placed on the detection

bench located outside the vacuum tanks.

4. Summary

The Frequency Control System is expected to suppress the frequency noise to a level of $\sim 10^{-4} \text{ Hz}/\sqrt{\text{Hz}}$ at 20 Hz rolling off to below $6 \times 10^{-6} \text{ Hz}/\sqrt{\text{Hz}}$ above 1 kHz. In order to maintain the full sensitivity a tight alignment control of the cavity is required. The overall control design has been developed and will be tested shortly.

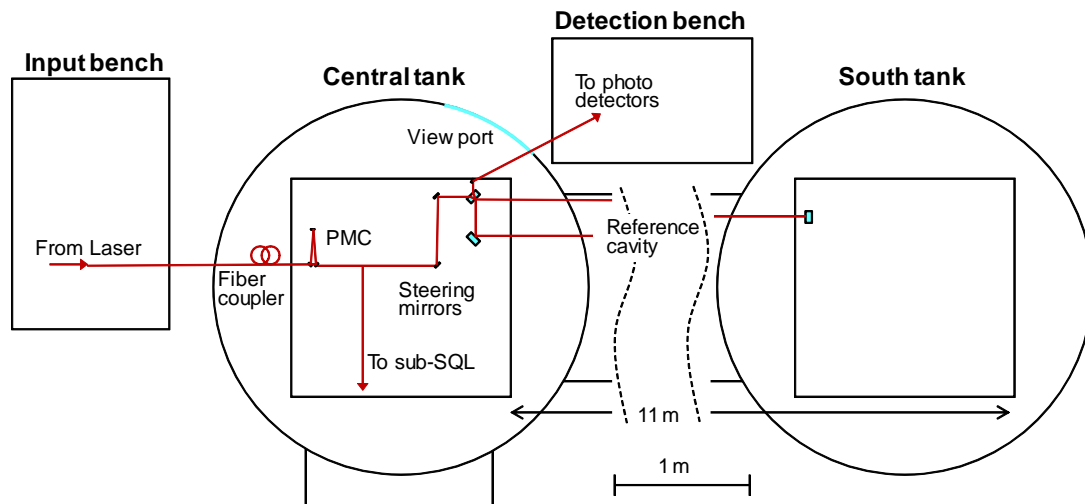


Figure 8. Optical layout of the reference cavity.

References

- [1] Gossler S *et al* 2010 *Class. Quantum Grav.* **27** 084023
- [2] Dahl K *et al* 2010 *J. Phys.: Conf. Series* **228** 012027
- [3] Kawazoe F *et al* 2010 *J. Phys.: Conf. Series* **228** 012028
- [4] Frede M, Schulz B, Wilhelm R, Kwee P, Seifert F, Willke B and Kracht D 2007 *Opt. Express* **15** 459
- [5] Kwee P and Willke B 2008 *Appl. Opt.* **47** 6022
- [6] Morrison E, Meers B J, Robertson D I and Ward H 1994 *Appl. Opt.* **33** 5041
- [7] Kawazoe F, Schilling R and Lück H 2011 *J. Opt.* **13** 055504